Development and application of cryo-EM tools to study the ultrastructure of microbes in changing environments

Depelteau, J.S.

Citation

Depelteau, J. S. (2022, January 12). *Development and application of cryo-EM tools to study the ultrastructure of microbes in changing environments.* Retrieved from https://hdl.handle.net/1887/3249707

Version:	Publisher's Version
License:	Licence agreement concerning inclusion of doctoral thesis in the Institutional Repository of the University of Leiden
Downloaded from:	https://hdl.handle.net/1887/3249707

Note: To cite this publication please use the final published version (if applicable).

CHAPTER 2

Bacterial and Archaeal Cell Structure

This chapter is published as:

Jamie S. Depelteau[1], Susanne Brenzinger[1], and Ariane Briegel[1]. (2019) Bacterial and Archaeal Cell Structure, Editor(s): Thomas M. Schmidt, Encyclopedia of Microbiology (Fourth Edition), Academic Press, Pages 348-360.

[1]Institute of Biology Leiden, Leiden University, Leiden, Netherlands

Abstract

The intricate nature of the cellular structure in bacteria and archaea has historically been underappreciated because of their small size. However, the advent of new microscopy techniques, such as fluorescent microscopy, super resolution light microscopy, cryo-electron microscopy, electron cryotomography and correlative microscopy techniques now enables the study of intact microbial cells at unprecedented resolution. We are now able to directly observe microbial cell structures and gain insight into essential processes such as establishing the proper cell shape, cell growth, division, motility, sensing and interacting with the environment and the formation of cellular communities. In this article, we will give a brief overview into the components of bacterial and archaeal cells, and how the cells rely on these structures to thrive.

Cell Boundaries of Microorganisms

Most bacteria and archaea constantly face changing and often hostile environments. Therefore, their cell envelopes must provide adequate protection against physical, chemical, and biological stresses while allowing an adequate influx of nutrients and efflux of waste products and signaling molecules. As bacterial and archaeal cell envelopes differ fundamentally in their composition and structure, they will be discussed separately.

Bacterial Envelope Structure

Traditionally, bacterial envelopes are classified into one of two groups using the Gram strain. Gram-negative bacteria possess a cytoplasmic membrane (CM), a thin peptidoglycan (PG) layer and an outer membrane (OM), while Gram-positive bacteria lack the OM and produce a thicker PG cell wall (Fig. 1, upper panel). Some notable exceptions of bacteria that lack a continuous PG layer exist, such as in *Mycoplasma*. The CM of bacteria is a phospholipid bilayer, its two leaflets are clearly distinguishable using electron microscopy at high magnification (Fig. 1, lower panel). The CM is water-permeable but impermeable to polar organic solutes and inorganic ions. This allows the cells to generate an inward-directed proton motive force, which is used to facilitate essential processes such as ATP syntheses and motility. Accordingly, a multitude of proteins involved in energy production, transport and secretion are embedded in the CM.

The major stress-bearing component of most bacteria is the PG network that envelopes the cell. PG is composed of long glycan strands of alternating N-acetyl glucosamine and N-acetyl muramic acid molecules which are crosslinked by short peptide chains. The CM and the PG are separated by a 10–20 nm wide space. In Gram-positive and -negative bacteria, the PG is similar in chemical composition and synthesis, but the PG layer of Gram-positive bacteria is substantially thicker (B40 nm) than in Gram-negatives. Lipoteichoic acids associated with the CM, teichoic acids and polysaccharides, which are linked to the PG, extend through the peptidoglycan network and form a negatively charged, loose outer layer. In Gram-negative bacteria, the PG is a B4 nm thin single layered mesh. The glycan strands run in a circumferential fashion around the cell body and the peptides roughly parallel to the long axis of the cell (see Fig. 2). While the PG of Gram-positive cells is generally much thicker than that of Gram-negatives, the thickness does not serve as a reliable phylogenetic
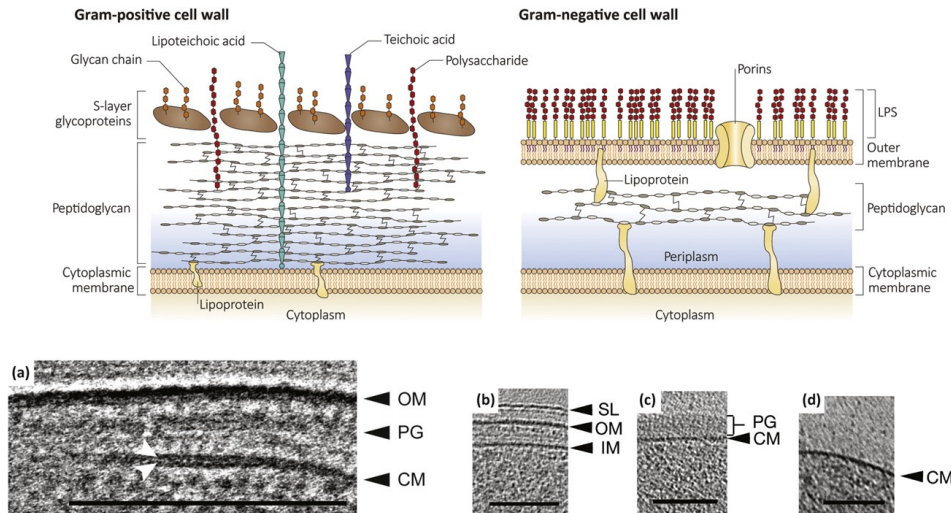
Figure 1. (Upper panel) Schematic side view of cell envelopes of exemplarily Gram-negative and -positive bacterial cells. LPS, Lipopolysaccharides. (Lower panel) Electron micrographs show the architecture of a Gram-negative cell wall without S-layer showing the two leaflets of the cytoplasmic membrane (white arrows): (a) *Vibrio cholera*; a Gram-negative envelope with S-layer: (b) *Caulobacter crescentus*; Gram-positive cell wall: (c) *Listeria monocytogenes*; cell-wall less: (d) *Mycoplasma pneumonia*. IM, inner membrane; OM, outer membrane; PG, peptidoglycan; SL, S-Layer; CM, cytoplasmic membrane; LPS, Lipopolysaccharides. Scale bars, 100 nm. Upper Panel reproduced from (13). Lower panel (a) courtesy of Wen Yang; (b-d) reproduced (14).

marker as several species possess intermediate thicknesses, and Gram-negative and -positive staining organisms may be found in the same class. Furthermore, the thick PG layer of *Bacillus subtilis* and *Acetonema longum* is converted to a thin layer reminiscent of the PG of Gram-negative bacteria during then initial stages of sporulation. The PG layer in Gram-negative bacteria is enclosed by the OM. The OM itself differs chemically from the CM as it is composed of an inner leaflet and an exterior leaflet of lipopolysaccharides (LPS) that provide the cell with a negatively charged barrier.

Some Gram-positive and -negative bacteria produce an additional proteinaceous surface layer on top of the PG layer or OM, respectively. This S-layer is mostly composed of one protein that self-assembles into oblique, square, or hexagonal lattice symmetries. Since the S-layer proteins arrange into a two-dimensional crystal in vitro, they can readily be studied by electron microscopy (Fig. 3). Finally, the outmost layer of many Gram-positive and -negative bacteria is a thick capsule of vastly variable polysaccharide associated with the OM or PG. This capsule provides additional protection against desiccation and is of clinical relevance as it facilitates cell attachment and evasion of the host immune defense.
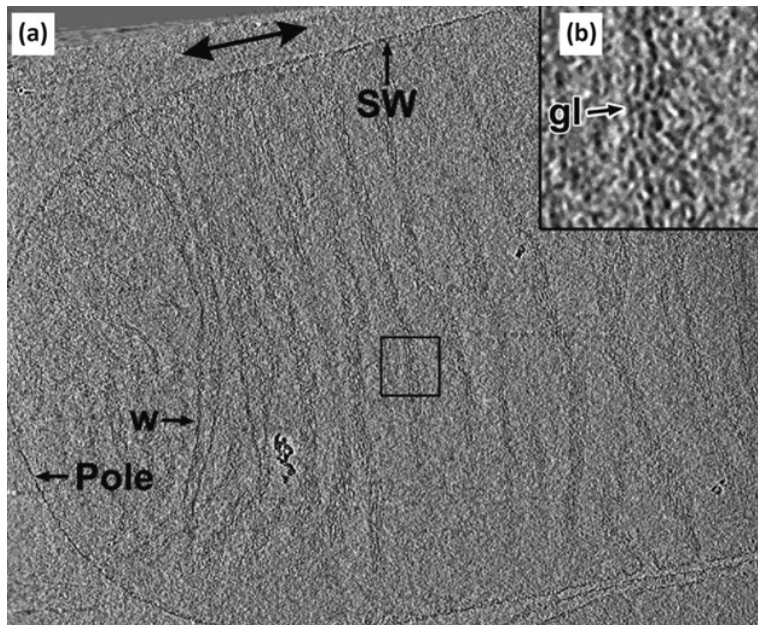
Figure 2. (a) Tomographic slices of *E. coli* XL-10 sacculus. Abbreviations: (gl) glycan strand; (SW) side wall; (w) wrinkle. (b) A four-fold enlarged view of the boxed region showing the glycan strands of the sacculus. The double-headed arrow denotes the saccular polar axis. Reproduced from (15).
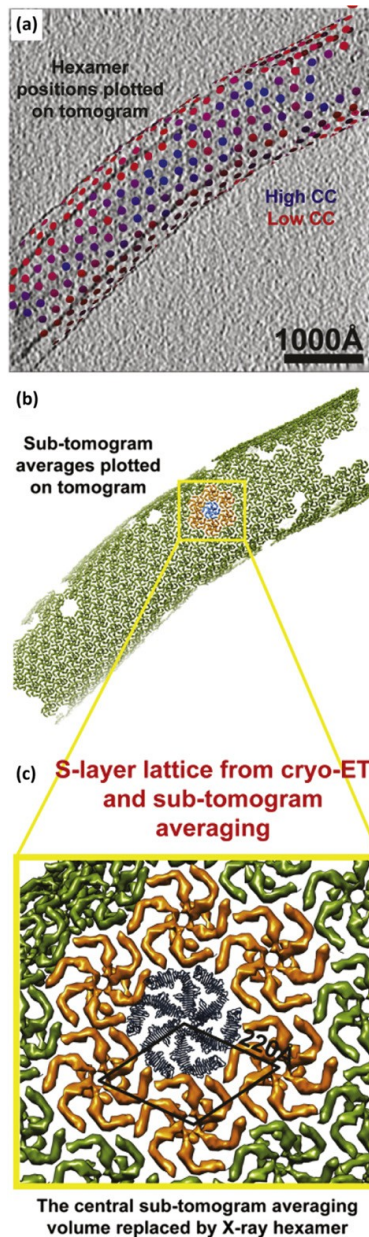
Figure 3. (a) Final refined positions of subtomograms of S-layer proteins plotted back onto a tomogram of a *C. crescentus* cell stalk with the corresponding refined orientations. Positions have been coloured from blue (high cross-correlation of alignment) to red (low cross-correlation). (b) The same plot as panel A, except each hexamer position is illustrated with the subtomogram average (green volumes). One hexamer is highlighted in blue, and the hexamers directly contacting it are shown in orange. (c) A zoomed view of the hexameric lattice revealed by cryo-ET and subtomogram averaging. The central blue hexamer from panel B is replaced by one copy of the X-ray hexamer. Reproduced from (16).

Archaeal Envelope Structure

While the chemical composition of CM, PG and OM is conserved among the bacteria, archaea produce a more diverse and species- specific set of envelope components (Fig. 4(a)). The lipids comprising the CM are unique for the archaea. Some species produce diether lipids that arrange into two leaflets whereas others possess tetraether lipids with up to 8 cyclopentane rings, thus forming a monolayer. Archaea also produce a variety of further structural components that envelope the CM. Some Euryarchaeota possess a cell wall composed of sugar polymers. However, unlike the PG of bacteria, archaeal cell walls differ vastly regarding their chemical composition and properties. Methanochondroitin for example is a fibrillar polymer that forms a rather loose matrix around aggregated cells. In contrast, pseudomurein has a thickness of approximately 15–20 nm and resembles PG in general architecture and rigidity. In most archaea that lack polymeric cell walls, an additional proteinaceous layer provides protection and maintains the cell shape. Most commonly, this is an S-layer with similar properties as their bacterial counterparts. However, while bacterial S-layers are only five to 20 nm thick, they may reach a thickness of up to 70 nm in archaea (Fig. 4(b)). Another type of protein layer is the tubular sheath of the filamentous growing *Methanospirillum* and *Methanosaeta* species. This sheath is composed of circumferential rings that envelope the entire filament. The circumferential hoops can clearly be seen using transmission electron microscopy (TEM). Capsule-like structures have been described for several archaea and genomic analysis suggests that many archaea encode genes for capsule systems.
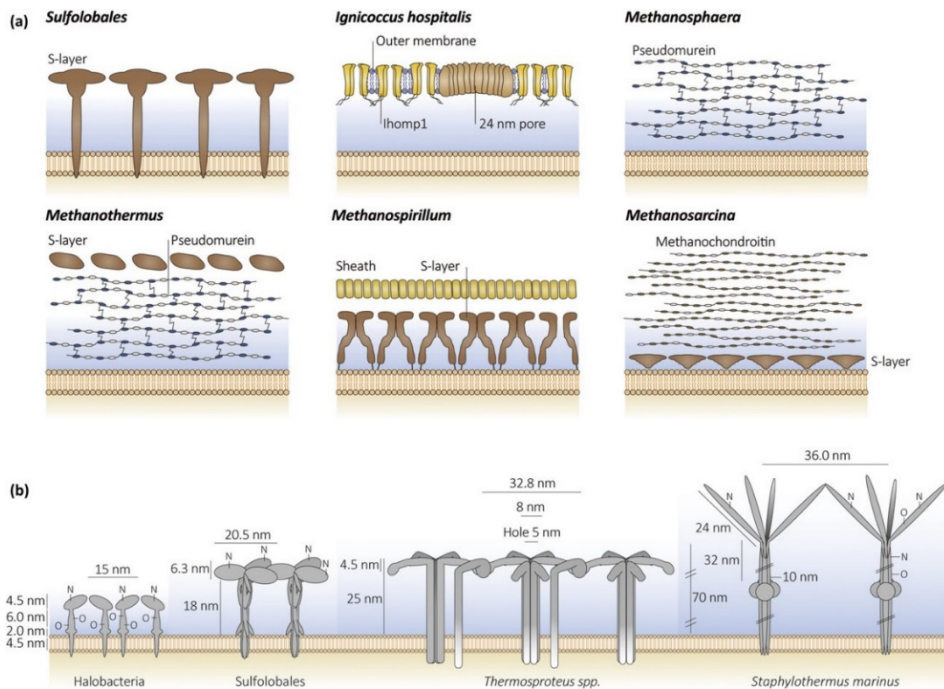
Figure 4. (a) Schematic side view of cell envelopes of exemplarily archaea. LPS, Lipopolysaccharides. (b) Models of the archaeal S-layer inside view. N, N-linked glycosylation; O; O-linked glycosylation. Reproduced from (13).

Cell Shape

Bacteria and archaea exhibit a broad diversity of cell shapes and cell sizes (Fig. 5). These features are tightly controlled through elaborate cell division machineries and structural features that maintain their intrinsic morphology. While some archaea share both structural and cell division components with bacteria, others have systems homologous to eukaryotic division machineries.

For most bacteria, the PG is both essential and sufficient to regulate and maintain their shape. However, how the PG synthesis is orchestrated to result in a particular shape is not well understood for most morphologies and organisms. In general, it is believed that cytoskeletal elements direct the PG synthesis machinery to the appropriate positions. In *Escherichia coli*, the actin-like cytoskeletal protein MreB coordinates localization of the PG synthesis machinery and, consequently, the insertion of PG precursors. MreB itself preferentially localizes to regions of negative curvature. The insertion of PG at these sites results in the growth of E. coli as a straight rod. In some cases, the cytoskeleton may play a more active role in shaping a cell. The vibrioid cell shape of *Caulobacter crescentus* is the result of crescentin, a

homologue to eukaryotic intermediate filaments. This protein coats the inner curvature of the cytoplasmic side of the CM. In contrast to coccoid spheres, alternative cell shapes offer the possibility of subcellular organization. In rod shaped cells for example the cell can distinguish between polar and midcell regions. In some bacteria, structures required for motility and chemosensing are predominantly found at one or both poles of the cell. The differently curved membrane at the pole can establish polarity of bacterial cells, and landmark proteins can recruit further proteins to the pole or protein gradients along the axis of the cell.

The cell shape maintenance in archaea is less well understood. CetZ, a protein related to eukaryotic tubulin and bacterial FtsZ, was shown to be essential for the development of rod-shaped *Haloferax volcanii* cells. This protein forms an additional layer underneath the membrane in cells producing high levels of this protein.
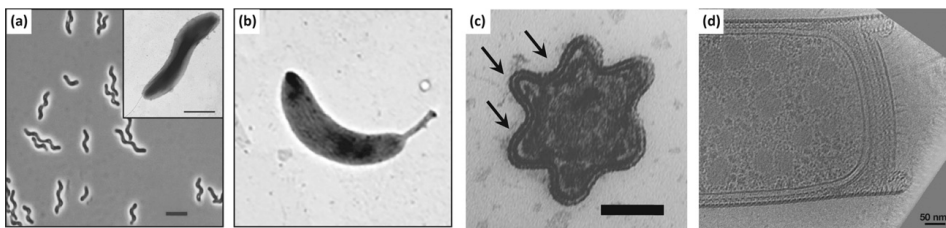

Figure 5. Diverse bacterial and archaeal morphologies. (a) Uncharacterized spiral-shaped methanotroph. Phase contrast with inset electron micrograph. (b) Transmission electron micrograph of *C. crescentus* (c) ultrathin section TEM micrograph of a six-pointed starshaped bacterium. (d) Cell tip of *Methanospirillum hungatei* cells imaged by cryo-electron microscopy. Modified from (a) (17), (b) (18), (c) (19), and (d) (20).

Cell Division

With few exceptions, the cell division machinery is necessary to reliably divide a cell into two daughter cells of similar volume and content. In nearly all bacteria, cell division is orchestrated by the tubulin homologue FtsZ. This specialized cytoskeletal element assembles into circumferentially orientated, overlapping filaments at the cytoplasmic side of the CM, which marks the division site and provides an assembly platform for the cell division machinery (Fig. 6). In Gram-positive bacteria, cell division occurs by septation. Here, the CM is pulled inwards and two new PG layers grow in parallel into the septum. At the outer rim of the septum, a PG bridge connects the old cell wall material of the mother cell both to each other as well as to new PG layers. Once septation is complete, the two daughter cells are fully

separated and split from each other. Division of Gram-negative bacteria follows a similar scheme with some variations. The constriction of the Gram-negative cell envelope starts either symmetrically, or asymmetrically at one side of the cell, before occurring circumferentially. Additionally, instead of forming a compact thin septum, the OM and PG lag behind the CM that moves into the center of the cell first, forming a V-shaped constriction. Here, the hydrolysis and synthesis of the PG bridge is speculated to be more controlled as it needs to move inward following the FtsZ ring while preventing premature rupture.

Archaea also divide by binary fission but exhibit a higher diversity of systems and modes of cell division than bacteria. Most *Euryarchaeota, Thaumarchaeota, Nanoarchaeota* and *Korarchaeota* encode an FtsZ-based division machinery, while the Cre- narchaeota possess a system homologous to the eukaryotic endosomal sorting complex required for transport III (ESCRT-III). Cell division of these archaea may occur either symmetrically or asymmetrically.
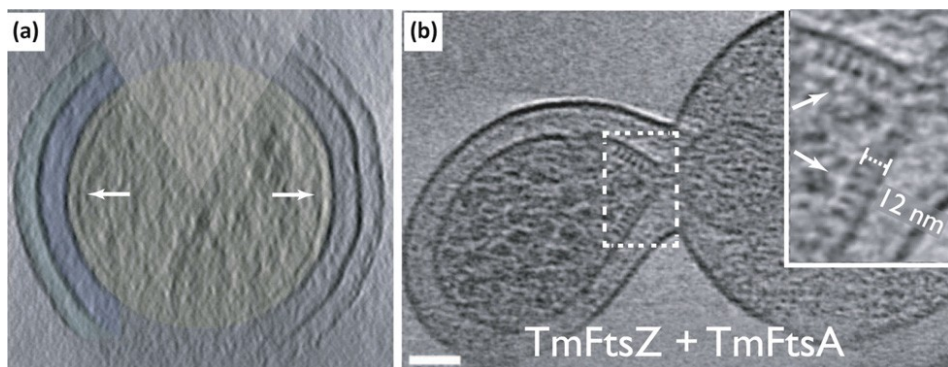
Figure 6. (a) FtsZ forms bands of filaments completely encircling *C. crescentus* NA1000/CB15N division site with filaments near the inner membrane IM. The Z ring (arrow) is continuous. The cytoplasm (beige), periplasm (blue), and space between the OM and S layer (cyan) have been colored for clarity. (b) 10-nm thick electron cryotomographic slice of an *E. coli* minicell formed from cells expressing Thermotoga maritima FtsZ and FtsA proteins, with a deeply constricted area showing cross-sections of FtsZ and FtsA filaments (black dots marked with white arrows). Distance between FtsZ filaments and IM is around 12 nm (inset in b). (a & b). Modified from (21).

Interaction with the Environment

Bacteria and archaea have developed an extraordinary arsenal of molecular machinery to interact with, as well as influence, the environment around them. The cells are able to sense their surroundings, determine the levels of nutrients, change the environmental milieu, and provide defenses for themselves and their neighbors. The following sections describe how bacteria and archaea interact with

their environment, highlighting the roles of motility apparatus, membrane vesicles, secretion systems, pili and, hami.

Motility

Some of the most striking structural features of bacteria and archaea are the proteinaceous ultrastructures required for cellular motility. Several distinct types of motility machineries have evolved in microorganisms, each adapted to a certain lifestyle and environment.

Swimming motility

Due to their small size, viscous forces are predominantly influencing microorganisms that move through water bodies. Therefore, reciprocal movements do not propel the cell. Bacteria and archaea solve this problem by using long rotating filaments that generate a fluid flow. Surprisingly, the bacterial flagellum and the archaeal archaellum have evolved separately, although they facilitate the same task.

The overall architecture of the flagellum can be divided into three major parts: The long helical filament extending from the cell body, a flexible hook and the envelope embedded basal body which comprises the rotary motor. Although the principal flagellar components are conserved among all flagellated bacteria, further proteins can modify the flagellar motor properties. Several additional periplasmic discs and ring structures are found to provide an increased structural support as well as a scaffold that allows more stators to be included in the motor. This results in increasing widths of the C- and stator ring (Fig. 7(a-i)). Both features allow cells to swim at a higher speed and torque.

Due to a similar assembly mechanism and homology of some components, the archaellum structurally resembles bacterial type IV pili (T4P) rather than the flagellum. Contrary to the flagellar filament, the archaellum is not hollow. Here, the prepilins are assembled into the pilus at the base of the growing archaellum. The motor is a multiprotein complex, however, rotation of the archaellum is powered by ATP hydrolysis and not by an ion-flux. While recent advances have elucidated the structure of the archaellum, several components and functions remain to be defined (Fig. 7(k and l)).
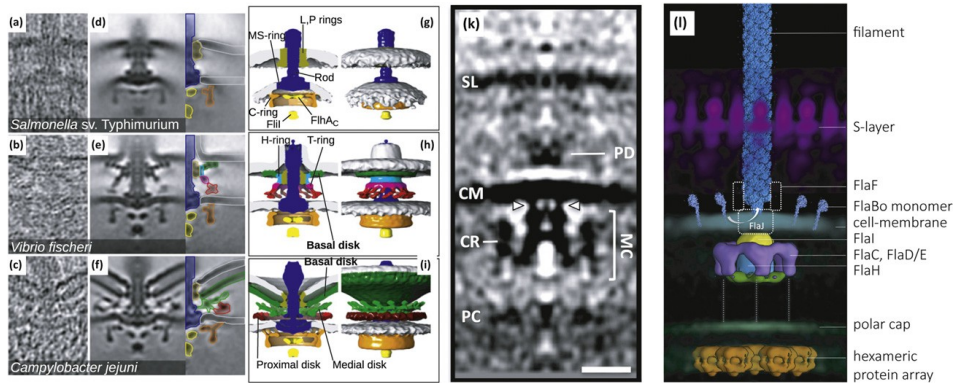
Figure 7. High-torque bacterial flagellar motors assemble large periplasmic disk complexes. (a–c) Tomographic slices through intact cells of *Salmonella* (a), *V. fischeri* (b), and *C. jejuni* (c) showing individual flagellar motors. (d-f) Slices (100 100 0.81 nm) through subtomogram averages of hundreds of motors. Color keys indicate the regions of the motor (named in g-i), (g-i) Isosurface renderings of motors shown in (d-f). FliI and FlhAC are components of the flagellar type III secretion system. (k) Tomographic slice through the subtomogram average of the motor complex of the archaellum of *Pyrococcus furiosus*. SL, S-layer; PD; periplasmic densities; CM, cell membrane; MC, motor complex; CR, cytosolic ring; PC, polar cap. Arrowheads indicate two of six narrow connections between MC and CM. (I) Composite model of the archaellum machinery of *P. furiosus*. Light blue, FlaB0 monomers and filament; hazy magenta, S-layer; solid yellow, blue, green, and purple, motor complex; hazy blue, cell membrane; hazy green, polar cap; solid orange, hexagonal protein array. Putative positions of protein subunits are indicated. Dashed grey lines, putative interaction with polar cap. (a-i). Modified from (22). (k & l) (23).

Surface Motility

Besides being required for attachment and biofilm formation, several bacteria possess retractile T4P that can attach to a surface and pull the cell towards the attachment point. This form of motility is referred to as twitching motility. Assembly of the pilus results in its extension, while the disassembly results in its retraction. Both processes depend on ATP hydrolysis. In several organisms, a specialized ATPase facilitates the depolymerization. Non-retractile and retractile T4P are structurally very similar.

An additional surface motility mechanism has been described for *Myxococcus xanthus*. The structural requirements of the so-called gliding motility, known as adventurous or A-motility, are not entirely understood. The current model of this mode of motility is based on the consecutive adhesion of OM lipoproteins to a surface, followed by the movement of the cell relative to that adhesion point, and the final release and disassembly of the lipoprotein complex at the lagging end of the cell. The involved protein complex appears to span the entire cell envelope. The release of a slime further facilitates the movement across the substratum.

Chemotaxis

In order to optimally benefit from the ability to move through the environment, many bacteria and archaea can sense their chemical environment and control their motility accordingly. This allows the cells to seek out their preferred environment and evade potentially harmful conditions.
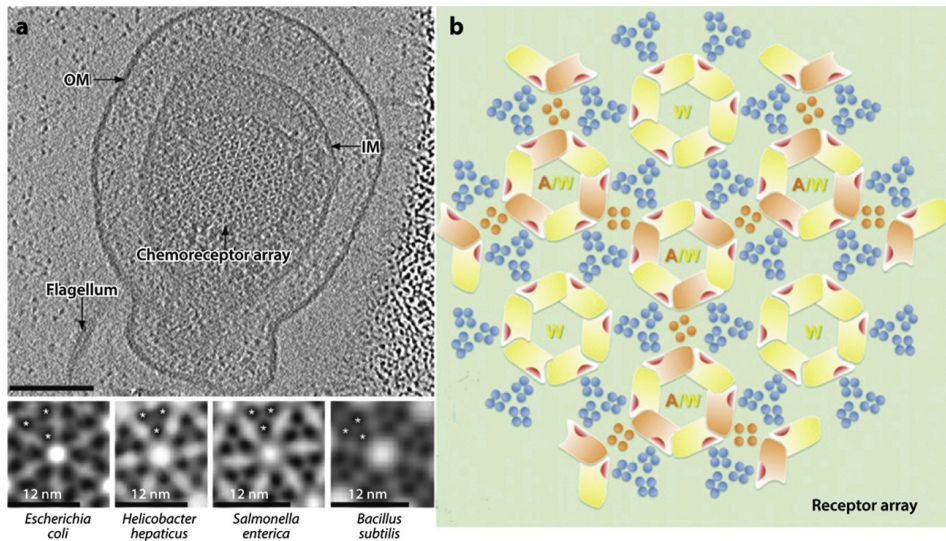
Figure 8. Visualization of the highly structured chemotaxis array by cryogenic electron microscopy (cryo-EM) in *Salmonella enterica* mini cells. (a) Viewed from the top, the chemotaxis array assumes a lattice formation (top) that is universal among bacteria (bottom). (b) Illustration of the chemotaxis array highlighting key proteins and their interacting partners that maintain the array: CheA (A, orange), methyl-accepting chemotaxis protein trimers (blue) and CheW (W, yellow). Scale bar in A (top) is 100 nm. Outer membrane (OM), inner membrane (IM). Modified from (24).

Chemotaxis is best understood in the model organism *E. coli*. Here, the cells can sense environmental cues such as sugars, amino acids or toxins via chemoreceptors that are anchored in the CM. The receptors, or MCPs (for Methyl accepting chemotaxis proteins), form trimer-of -receptor dimers, and these trimers are in turn arranged in highly ordered arrays, where six trimers form the corners of a hexagon (Fig. 8). This receptor packing, and thus the distance between the centers of the hexagons of 12 nm in the lattice, is highly conserved and universal across the bacteria and archaea.

In *E. coli*, the cytoplasmic tips of the receptors are networked by rings formed by the histidine kinase CheA and the linking protein CheW. CheA autophosphorylates and transfers this phosphoryl group to a messenger protein CheY upon an increase of repellents or a removal of attractants. The phosphorylated messenger protein CheY binds to the flagellar motors and biases the direction of flagellar rotation from

the default counterclockwise (CCW) to clockwise (CW). This results in a tumbling behavior where the cells randomly reorient their cell axis. Once all flagella of the cell return to CCW, the cells swim smoothly forward (run) in a new direction. The control of frequency and duration of these tumbles result in a biased random walk, which ultimately provides the means to find their preferred environment.

While *E. coli* only possesses one chemotaxis system, more than half of all chemotactic bacteria have additional chemotaxis systems encoded in their genome. Some of these systems lack the transmembrane and periplasmic regions of the receptors, and thus form purely cytoplasmic chemoreceptor arrays. Structurally, these arrays consist of two layers, where each layer is hexagonally packed like their membrane-bound counterparts. The receptors of both layers overlap and are sandwiched in between two layers composed of CheA and CheW. While we are beginning to understand the architecture of such cytoplasmic arrays, their function remains largely unclear.

Membrane Vesicles

Membrane vesicles are an essential component found in both Gram-positive and Gram-negative bacteria, as well as in archaea (also referred to outer membrane vesicles in gram negative bacteria). These vesicles are typically spherical, ranging in size from 20 to 100 nm in Gram-positive bacteria and archaea to 100–300 nm in Gram-negative bacteria (Fig. 9). The lipid bilayer composition of the vesicles resembles that of the membrane where the vesicle originated. They can contain cell-wall material, as well as a variable content enclosed by the membrane. In addition, the content of membrane vesicles can be enriched with a diverse set of molecules including LPS, peptidoglycan, nucleic acids, metabolites, and signaling molecules. The mechanism by which membrane vesicles are generated is still under investigation.
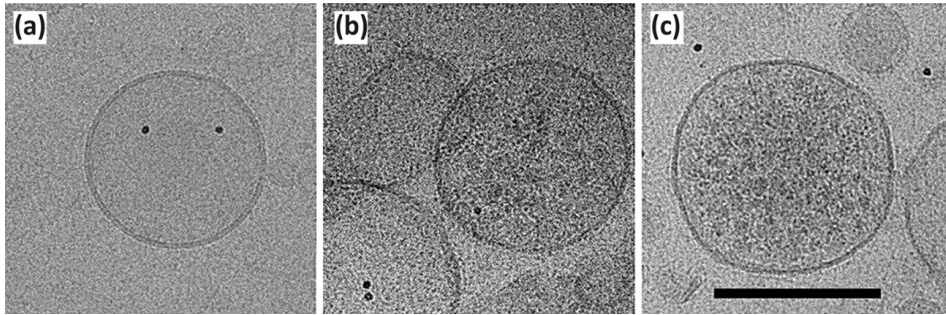
Figure 9. Cryo-EM of membrane vesicles isolated from *Streptomyces*, demonstrating the variety of sizes and variability in contents. Three types of vesicles are noted: Empty (a), partially filled, with or without external membrane complexes (b), or heavily filled with material (c). Scale bar 200 nm. Modified from (25).

Membrane vesicles have many proposed functions: bacterial communication, modulation of stressful environments, com- ponents for biofilm formation, and defense strategies. The membrane vesicles can be filled with specialized cargo that elicit specific types of response, including the recognition of self and non-self organisms. For the acquisition of nutrients, outer membrane vesicles (OMVs) can be filled with proteases and glycosidases, or with DNA and proteins that can be a source of food for the community. Recent studies have also demonstrated that interactions with specific hosts can bias the proteins found in membrane vesicles to those that are important to the bacteria-host relationship, including adhesions for binding to specific cell types. For instance, the Gram-positive bacteria Staphylococcus aureus produce membrane vesicles that contain beta lactamase as a way to protect the local environment from the antibiotic penicillin. In addition, membrane vesicles have also been shown to provide a defense against bacteriophage infection by acting as a decoy. Thus, membrane vesicles play an essential role in the bacterial and archaeal life cycle by modulating the environment in favor of their survival.

Secretion Systems

In addition to releasing membrane vesicles into the environment, bacteria and archaea have developed various mechanisms to transport unfolded or folded proteins across their membrane(s) and into the local environment or across the membrane of a target cell. Some systems allow a protein to move from the cytoplasm directly to the extracellular space in a one-step process. Others require several steps for the target protein to exit the cell via a transport system through the CM, followed by a second transport system that spans the OM and/or cell wall. Upon translocation, the proteins remain either attached to the cell envelope, are

released into the extracellular space, or are transferred directly into the target cell. Thus far, as many as sixteen unique complexes have been shown to be involved in protein transport across the membrane. Each system plays a specific role in bacterial and archaeal physiological processes. Furthermore, these systems are the primary method for the release of bacterial effector proteins that act on other cells in the environment. Some secretion systems are universal among bacteria and archaea, such as the Sec and Tat pathways, while others are restricted to a specific phylum or species. The same is true for the cargo of each system, some transporting a wide range of proteins and others are specific to just a small number of proteins. The secreted proteins have many roles in the bacterial and archaeal life cycle, including uptake of nutrients, expression of virulence factors, and attachment to target cells. Gram-negative bacteria have multiple secretion systems: Sec, Tat, type 1 secretion (T1SS), T2SS, T3SS, T4SS, T5SS, T6SS, and T9SS. Gram-positive bacteria have at least four systems, Sec, Sec2A, Tat, and T7SS, and only Sec and Tat have been identified in archaea so far. Because of the large number of secretion systems across bacteria and archaea, this section will highlight only those systems with significant ultrastructural information.

Type II Secretion System

The type II secretion system (T2SS) is only found in Gram-negative bacteria where it is responsible for secreting folded proteins from the periplasm through the OM. Proteins that are destined for the T2SS are first transported in an unfolded state across the CM by the Sec or Tat systems. Once in the periplasm, the protein is folded and then transported into the extracellular space by the T2SS. This secretion system is an important component in pathogenesis, and many pathogens utilize this pathway to deliver toxins to target cells. A well-studied example of this mechanism is the transport of the cholera toxin during *Vibrio cholerae* infection. The T2SS is thought to work by a piston mechanism, where the cholera toxin is mounted to a platform on the periplasmic side of the CM and then pushed through the OM pore. This export is powered by the retraction of the pseudopilins (Fig. 10).
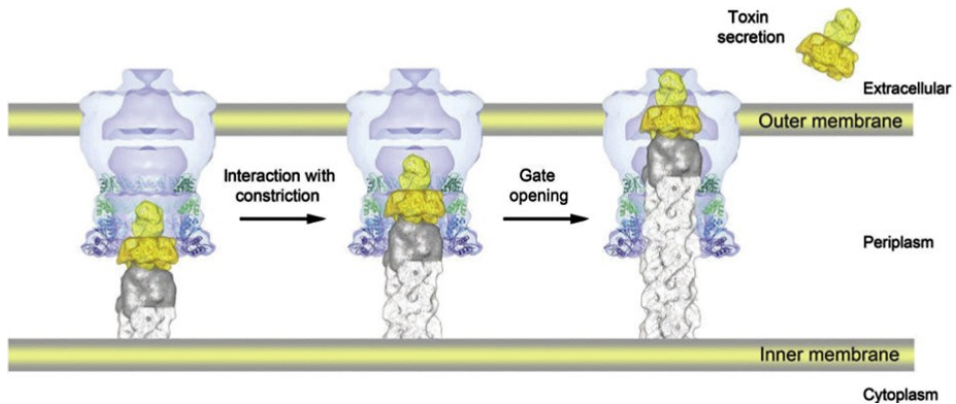
Figure 10. Schematic representation of the secretion of *V. cholerae's* cholera toxin by a piston-driven mechanism of the T2SS. Cholera toxin (gold) is loaded on the pseudopilus tip (grey). The toxin is then pushed into the periplasmic portion of the membrane channel by the extension of the pseudopilus. Secretion of the toxin is permitted by the opening of the membrane channel and continued growth of the pseudopilus. Modified from (26).

Type III Secretion System

The type III secretion system (T3SS) is also known as the injectisome because its structure resembles a needle and syringe and acts in a similar fashion. This system is found exclusively in Gram-negative bacteria, where it spans the whole cell envelope, as well as the membrane of its target cell. This provides the opportunity for the transport of unfolded proteins directly into the target cell. This transfer of bacterial effectors typically facilitates the creation of a more favorable environment for the delivering bacteria. Three main components of the T3SS have been characterized: the basal body, the needle and the translocon. The needle extends from the base into the extracellular space and consists of a hollow channel that permits transport of unfolded proteins. The translocon is responsible for the transport of effector proteins upon contact with the target cell. The T3SS has been structurally well characterized, and recent studies provided detailed insight into the structural variations of the T3SS in *Chlamydia* and *Salmonella* (Fig. 11).
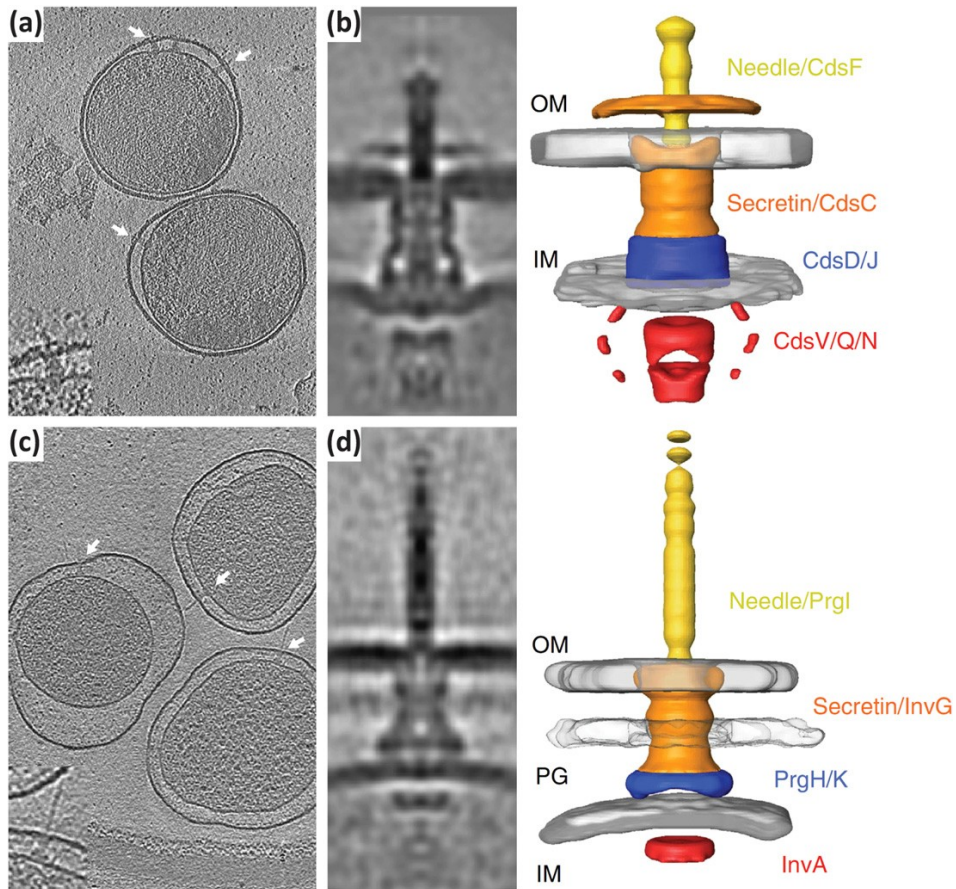
Figure 11. Cryo-EM visualization of the T3SS obtained from *Chlamydia trachomatis* elementary bodies (a, b) and Salmonella enterica minicells (c, d). The T3SS apparatus spans the inner and outer membranes (a, c; white arrows). Further image processing provides a detailed view of the T3SS structure (b, d) and can be represented by both electron micrographs (left) and 3D surface rendering (right). OM – outer membrane, PG – peptidoglycan, IM – inner membrane. Scale bars, 200 nm (a, c) and 15 nm (b, d). Modified from (27).

Type IV Secretion System

The function of the type IV secretion (T4SS) system is used for bacterial conjugation, where it enables the cells to secrete a wide variety of molecules including single stranded (ss) DNA and ssDNA-protein complexes directly into a target cell. There are two types of T4SS: the retractable T4aSS and the non-retractable T4bSS. The T4SS spans the CM and OM of Gram-negative bacteria as well as the membrane of the target cell. The secretion system provides the means to export and import DNA, and thus contributes to spread of antibiotic resistance genes. The structure of the T4SS is similar across all identified T4SS variants, though the role of an extracellular pilus in some systems is still unknown. This system is important for virulence in

many bacteria, such as in the pathogen *Legionella pneumophila*, where the structure of this T4bSS has been recently solved (Fig. 12). In this organism, the T4bSS transports effectors into the target cells in order to disrupt the host's defense, and thus enabling bacterial colonization.
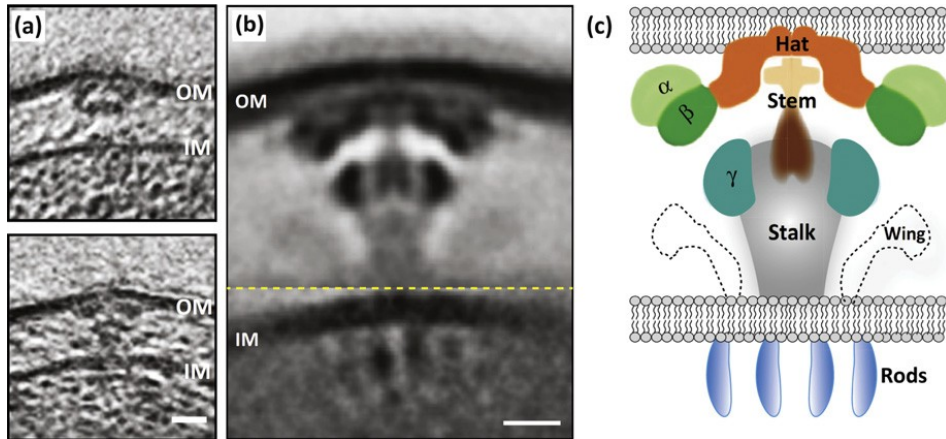
Figure 12. Cryo-EM and advanced image processing reveal the in vivo structure of the T4bSS of *Legionella pneumophila*. The T4bSS spans the outer and inner membrane (OM, IM) of the cell (a) Subtomogram averaging clarifies the structural features (b) and is fitted with known protein components that comprise the complete T4bSS structure (c) Scale bars: 20 nm (a) and 10 nm (b) Modified from (28).

Type VI Secretion System

Similar to the T3SS, the type VI secretion system (T6SS) transports proteins from the bacterial cytoplasm directly into the target cell. Found only in Gram-negative bacteria, this system is thought to be both a form of communication and competition among various bacteria. The T6SS secretes bacterial toxins either into other bacterial cells in the local environment, or into eukaryotic cells. The T6SS is highly efficient in protein transport, and it provides the cells with both defensive and offensive protection against other bacteria that also employ the T6SS. In addition, this system has been implicated in bacterial response to stress and for self-recognition. Furthermore, it contributes to horizontal gene transfer, since it uses this system to kill opponent cells. The resulting lysis frees the DNA that can subsequently be taken up by other secretion systems.
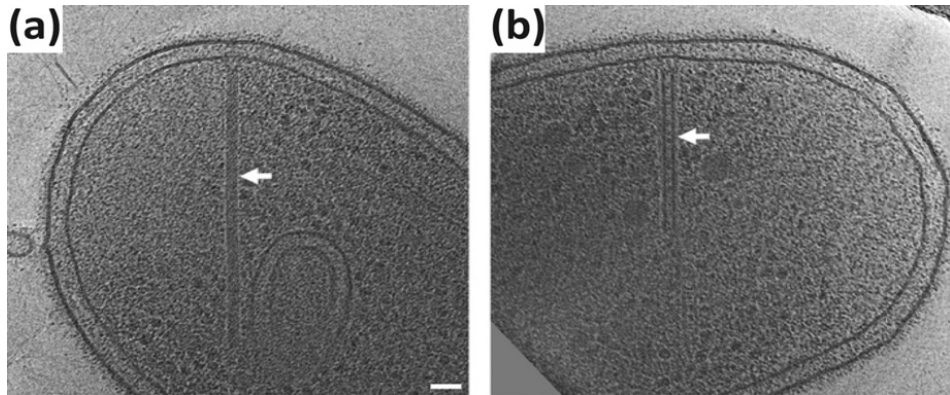
Figure 13. Visualization of the T6SS in vivo by cryo-EM. The T6SS in the extended (a) and contracted state (b) in *Myxococcus xanthus*. The extended version spans a significant portion of the cell and once triggered contraction delivers effectors to the target cell. Scale bar: 50 nm. Modified from (29).

The T6SS is homologous to the tail structure found in bacteriophages. Structurally, the base of the T6SS is anchored to the CM, and upon contraction of a sheath-like structure, the inner tube is propelled into a target cell, puncturing the target cell's membrane with a spike-like protein tip. A well-studied structural model for the T6SS comes from *M. xanthus*. In this organism, the T6SS is characteristic tube-shaped structure within the cell (Fig. 13(a)). The tube structure is extended into the cytoplasm and anchored to the CM. Upon external trigger the sheath of the tube constricts propelling bacterial effectors into the target cell. In the bacterium *Pseudoalteromonas luteoviolacea*, a structured termed the MAC complex induces metamorphosis in tube worms. Here, the T6SS form a large array of tubes held together by a protein mesh, that are released into the environment and act as 'land mines' that induce the metamorphosis of the tube worm.

External Appendages

Pili (Also Known as Fimbriae)

Bacteria and archaea have evolved a number of external appendages that can be used for attachment, secretion, electron uptake, and motility. Such structures include four types of pili. Gram-positive and Gram-negative bacteria have similar types of pili, however their fine structures differ. The chaperone-usher pili are mainly found in Gram-negative bacteria and are used for host attachment and virulence. Chaperone-usher pili are typically 1–2 mm in length with the pilin subunits arranged in a helical pattern. This pilus architecture provides the ability to stretch.

In addition to the functions mentioned for the chaperone-usher pilus, the type 4 pilus (T4P) is also involved in twitching and gliding motility. T4P can be several microns in length with a diameter of 6–9 nm. T4P are unique among the pili because some variants have the ability to extend and retract, which provides the means for the cell's motility. During assembly, pilins are removed from the CM and assembled in the periplasmic space by the T4P basal body, causing the filament to extend out into the extracellular space. There are two types of T4P, Type IVa (T4aP) and Type IVb (T4bP). T4aP has a range of functions including cell motility and DNA transfer, while T4bP is specifically used for host colonization. The Gram-negative organism

V. cholerae has a unique, well-studied form of the T4bP called the toxin co-regulated pili (TCP). The TCP is essential to the *V. cholerae* infection cycle, providing a means of attachment for the bacterium when it enters the mucosal regions of its host. Additionally, it enables the cells to form microcolonies. The different T4P types are remarkably similar in composition and structure, though only T4aP have the ability to retract (Fig. 14). TcpA is the major pilin subunit for both systems, which forms the extracellular appendage.
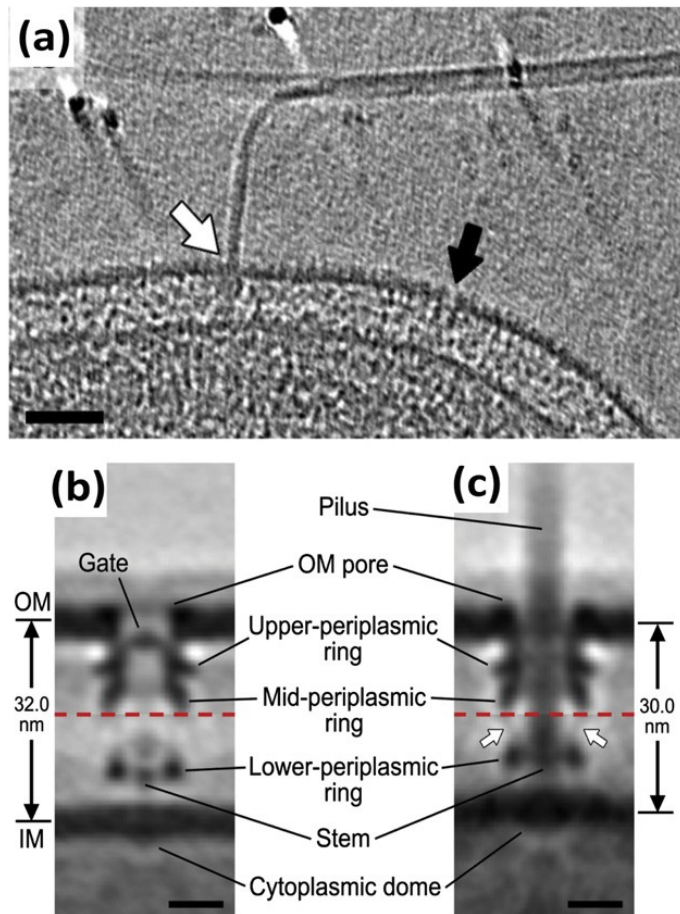
Figure 14. T4P. *V. cholerae* exhibits a unique type IV pilus apparatus called the toxin-co-regulated pilus machine (TCPM). A. Using cryo-EM, the piliated TCPM (white arrow) and non-piliated basal body (black arrow) are identifiable on the cell surface. Image processing enables the user to gain greater detail of the TCPM allowing the comparison of the piliated (b) and non-piliated states (c). Scale bars: 50 nm (A), 10 nm (B, C). Modified from (30).

The conjugative T4P pilus, also called F-pilus or F-like pilus, is the primary method used between bacteria for the transfer of genetic information. This structure is present only in Gram-negative bacteria and requires a specific plasmid that codes for the essential components of this conjugative pilus. This system is unique as it requires the use of a T4SS for assembly. The current model of this system is that once two cells are connected, the pilus is retracted in order to bring the two cells together, thus allowing for the transfer of genetic material.

Lastly, the type 5 pili (T5P) are unique to the *Bacteroides* phylum, consisting of two types of pilin appendages: a long pilus that extends approximately 0.3–1.5 mm from

the cell body, whereas the short pilus is restricted to 80–120 nm. This pilus type has several roles including adhesion, aggregation, biofilm formation, and virulence.

Other Cell Attachment Structures

Hami

Some archaea, such as the *Candidatus Altarchaeum hamiconexum*, have an additional, unique appendage that is used for attachment to surfaces, other cells, as well as important in biofilm formation in extreme environments. Upwards of a hundred of these pilus- like structures extend from the cell surface, with each hamus having a diameter of 6–8 nm and protruding several microns into the environment. The hami are made of three intertwined filaments. The hamus terminates in a characteristic tripartite structure that resembles a grappling hook (Fig. 15). Many hami have three barbs emerging approximately 47 nm apart along the main thread. The assembly of this structure is thought to be mediated by the Sec pathway, moving the three subfilaments into the periplasm for hamus assembly. However, the filaments are not related to known bacterial filaments and recent research suggests that it may have evolved from modified S-layer proteins.
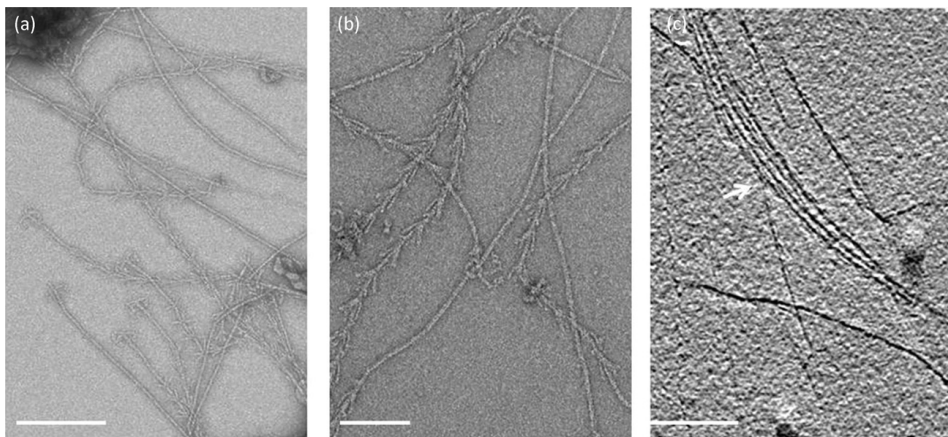
Figure 15. The archaeal hami of *Candidatus Altiarchaeum hamiconxeum* visualized by negative stain EM (a, b) and cryo-electron tomography (c) demonstrating the characteristic barbed structure filament with tripartite tips. Scale bar: 500 nm. Reproduced from (31).

Further Reading

Adams, D.W., Errington, J., 2009. Bacterial cell division: Assembly, maintenance and disassembly of the Z ring. Nature Reviews Microbiology 7 (9), 642–653. doi:10.1038/ nrmicro2198. (32)

Albers, S.-V., Meyer, B.H., 2011. The archaeal cell envelope. Nature Reviews Microbiology 9 (6), 414–426. doi:10.1038/nrmicro2576. (13)

Briegel, A., Jensen, G., 2017. Progress and potential of electron cryotomography as illustrated by its application to bacterial chemoreceptor arrays. Annual Reviews of Biophysics 46, 1–21. doi:10.1146/annurev-biophys-070816-033555. (24)

Caccamo, P.D., Brun, Y.V., 2018. The molecular basis of noncanonical bacterial morphology. Trends in Microbiology 26 (3), 191–208. doi:10.1016/j.tim.2017.09.012. (33)

Chang, Y., Kjaer, A., Ortega, D., et al., 2017a. Architecture of the *Vibrio cholerae* toxin-co-regulated pilus machine revealed by electron cryotomography. Nature Microbiology 2, 16269. doi:10.1038/nmicrobiol.2016.269. (30)

Chang, Y., Rettberg, L.A., Ortega, D.R., Jensen, G.J., 2017b. In vivo structures of an intact type VI secretion system revealed by electron cryotomography. EMBO Reports 18 (7), 1090–1099. doi:10.15252/embr.201744072. (29)

Ghosal, D., Chang, Y., Jeong, K.C., et al., 2017. In situ structure of the *Legionella* Dot/Icm type IV secretion system by electron cryotomography. EMBO Reports 18 (5), 726–732. doi:10.15252/embr.201643598. (34)

Green, E.R., Mecsas, J., 2015. Bacterial secretion systems: An overview. Microbiology Spectrum 4 (1), doi:10.1128/microbiolspec.VMBF-0012-2015. Harshey, R.M., 2003. Bacterial motility on a surface: Many ways to a common goal. Review of Microbiology 57 (1), doi:10.1146/micro.2003.57.issue-1. (35)

Hospenthal, M.K., Costa, T.R.D., Waksman, G., 2017. A comprehensive guide to pilus biogenesis in Gram-negative bacteria. Nature Reviews Microbiology 15, 365–379. doi:10.1038/nrmicro.2017.40. (36)

Kearns, D.B., 2010. A field guide to bacterial swarming motility. Nature Reviews Microbiology 8 (9), 634–644. doi:10.1038/nrmicro2405. (37)

Kim, J.H., Lee, J., Park, J., Gho, Y.S., 2015. Gram-negative and Gram-positive bacterial extracellular vesicles. Seminars in Cell & Developmental Biology 40, 97–104. doi:10.1016/j.semcdb.2015.02.006. (38)

Nans, A., Kudryashev, M., Saibil, H.R., Hayward, R.D., 2015. Structure of a bacterial type III secretion system in contact with a host membrane in situ. Nature Communications 6, 10114. doi:10.1038/ncomms10114. (27)

Perras, A.K., Daum, B., Ziegler, C., et al., 2015. S-layers at second glance? Altiarchaeal grappling hooks (hami) resemble archaeal S-layer proteins in structure and sequence. Frontiers in Microbiology 6, 543. (31)

Reichow, S.L., Korotkov, K.V., Hol, W.G.J., Gonin, T., 2010. Structure of the cholera toxin secretion channel in its closed state. Nature Structural & Molecular Biology 17 (10), 1226–1232. doi:10.1038/nsmb.1910 1226. (26)